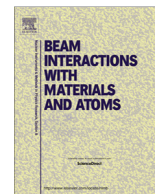




Contents lists available at ScienceDirect

Nuclear Instruments and Methods in Physics Research B

journal homepage: [www.elsevier.com/locate/nimb](http://www.elsevier.com/locate/nimb)

## Spatial distribution of PXR generated by 855 MeV electrons: Comparison of simulation results with experimental data

Yu. A. Goponov<sup>a</sup>, M.A. Sidnin<sup>a</sup>, I.E. Vnukov<sup>a</sup>, C. Behrens<sup>b</sup>, G. Kube<sup>b</sup>, W. Lauth<sup>c</sup>, A.S. Gogolev<sup>d,\*</sup>, A.P. Potylitsyn<sup>d</sup>

<sup>a</sup>Belgorod National Research University, Belgorod, Russia

<sup>b</sup>DESY, 85 Notkestr. 22607 Hamburg, Germany

<sup>c</sup>Institut für Kernphysik, 45 Johann-Joachim-Becher-Weg, 55128 Mainz, Germany

<sup>d</sup>National Research Tomsk Polytechnic University, Tomsk, Russia

### ARTICLE INFO

#### Article history:

Received 29 November 2016

Received in revised form 2 March 2017

Accepted 2 March 2017

Available online xxxx

#### Keywords:

Beam diagnostics

Parametric X-ray radiation

Accelerator

Crystal

### ABSTRACT

The detailed data treatment of the experiment performed in MAMI-B microtron with the X-ray camera, taking into account the contribution of both diffracted transition radiation and bremsstrahlung, is presented. The X-ray camera efficiency was additionally considered. The simulated emission pattern in general agrees with the experimental one. However, along the Bragg direction where the influence of the beam size on the emission spatial distribution is most noticeable, a discrepancy between the model and the experiment is observed. Possible reasons of such discrepancy are discussed.

© 2017 Published by Elsevier B.V.

### 1. Introduction

Invasive [1] and noninvasive [2,3] methods for estimation of the transverse beam size based on registration of optical radiation from metal foils set in the accelerator can't ensure measurement of the beam parameters with sizes about some tens of nanometers because of coherent effects in the radiation [4]. Microbunching instabilities in high-brightness electron beams of modern linac-driven free-electron lasers (FELs) can lead to coherence effects in the emission, thus making it impossible to obtain a direct image of the particle beam, especially for transverse beam profiles. To allow beam profile measurements for small beam size and in the presence of microbunching instabilities, different monitor concepts are considered.

Parametric X-ray radiation (PXR) in thin crystals can be used for this purpose [5,6]. PXR is emitted when a relativistic charged particle beam crosses a crystal, and the radiation process can be understood as diffraction of the virtual photon field associated with the particles at the crystallographic planes.

Studies on the influence of the electron beam size on the PXR spatial distribution from electrons with an energy of 855 MeV in the silicon crystal thickness of 50  $\mu\text{m}$  using a high-resolution

X-ray camera [7] (HRC) based on a thin scintillator coupled waveguides with CCD matrix in experiment [8] confirmed the possibility of estimation of the electron beam size with the help of such measurements.

Using PXR or any other mechanism of radiation to determine the size of an electron beam is possible if we have a good agreement between measured and calculate angular distribution for a point such as an electron beam spot.

Results by already cited work [8] are not described by PXR kinematic theory. At the distribution centre, where the influence of beam size on the radiation spatial distribution is most noticeable, a large difference between the experimental result and kinematic theory prediction was observed [8]. A gap in the centre of the PXR angular distribution which was predicted by PXR theory and usually observed for thin crystals, see, for example [6,9], occurred very small.

Considering the real photon diffraction for the [8] experiment, an improved correlation between the experimental and calculated data was obtained for the centre of PXR reflex [9]. However, the difference between the experimental and calculation results remains relatively large. Based on what is mentioned above, it is important and relevant to compare the experimental results [8] with calculation taking into account the influence of all experimental conditions more carefully than it was made in Ref. [9] and try to find the reason of the discrepancies observed.

\* Corresponding author.

E-mail address: [gogolev@tpu.ru](mailto:gogolev@tpu.ru) (A.S. Gogolev).

## 2. Calculation

In the general case in the experiment, all the mechanisms of radiation generation at the Bragg angles are implemented simultaneously; therefore, in comparing experimental results with calculated ones, it is necessary to consider all types of radiation. The kinematic PXR theory describes the results of measurements quite well [10], therefore, the PXR yield was calculated using a PXR spectral-angular distribution formula obtained in the kinematic approximation [11].

For high-energy electrons, the radiation in the X-ray range of photon energy ( $\omega \leq 100$  keV) in crystals, except PXR, is generated through the mechanism of the diffracted transition radiation (DTR) and the diffracted bremsstrahlung (DB). The methods of the PXR, DTR, and DB yields calculation, taking into account the electron beam divergence and multiple scattering in the crystal, the emission collimation angle and other experimental conditions are described in detail by Laktionova et al. [9].

The main purpose of this study is to explain the results of the experiment [8], where the PXR kinematic theory does not describe the measurements results without considering the contribution of real photon diffraction and accurate inclusion of the experimental technique characteristics. To analyse the influence of the diffracted real photon contribution and experimental conditions on the angular distribution of the resulting radiation, a series of calculations of radiation yield for the experimental conditions [8] and the (004) reflection order were performed with procedure [9].

The rectangular detector, the size of which is  $77.28 \times 80.04 \mu\text{m}^2$ , is moving down through the centre of reflex vertically with a step of  $77.28 \mu\text{m}$ , which corresponds to the angular distribution measurement using an X-ray camera with a pixel size of  $11.2 \times 11.6 \mu\text{m}^2$  for angular capture  $3 \times 3$  pixel and relation between CCD size and the camera field of view  $\approx 2.3$  [7] (see the next section).

Fig. 1a shows the vertical spatial distributions of PXR, DTR, and DB for the first-order reflection calculated by a technique [9], so these are curves 1–3, respectively. Curve 4 is the distribution for all emission mechanisms PXR + DTR + DB. From the figure, it is seen that PXR has a bigger intensity than DB and DTR, and its angular distribution is broader. In the centre of PXR angular distribution, there is a broad failure, whereas the output of DTR and DB is concentrated near Bragg's direction. Thus, the diffracted photon yield gives the main contribution into the radiation yield in the reflex centre. As can be seen from the figure, DTR spatial distribution has a failure in the centre too. However, it is narrower than that of PXR; therefore, spatial distribution of the total radiation yield possesses a narrower minimum than PXR one. The energy

of photons of the first allowed reflection order is  $\omega = 23.4 \text{ keV} < \gamma\omega_p \approx 50 \text{ keV}$ , which is why the yield of diffracted Bremsstrahlung is suppressed because of the Ter-Mikaelian effect of density [12] and appears to be less than the DTR yield.

As it was remarked in [9], HRC measures the combined angular distribution for all reflection orders rather than for individual orders. Fig. 1b shows the vertical spatial distribution of total radiation PXR + DTR + DB for three orders of reflection calculated by a technique [9], considering the spatial size of the electron beam on the crystal, so these are curves 1–3, respectively. It is supposed that the beam spatial distribution is Gauss one with  $\sigma_x = \sigma_y = 50 \mu\text{m}$ . Curve 4 is the first-order total radiation spatial distribution calculated for a point such as the electron beam.

From the figure, it is seen that the first-order reflection has maximum intensity. The contributions of the second and particularly the third and subsequent orders with higher-energy photons and narrower angular distributions are substantially less. However, the second-order contribution is still significant, and with the help of an absorber in the photon beam between the crystal and the detector, as in the analysed experiment [8], can be comparable with the contribution of the first-order reflection. It should be remarked that following reflection orders have spatial distributions with less depth than the first one. From comparison between calculation results with and without influence of spatial beam size (curve 1 and curve 4 respectively), it is seen that it is concentrated in the distribution centre and decreases the depth of the failure for the first reflection order in approximately 1.5 times.

## 3. Experimental setup

The analysed experiment [8] was performed at the 855 MeV beam of the Mainz Microtron MAMI (University of Mainz, Germany) in the beamline of the X1 collaboration. Fig. 2 shows a sketch of the experimental setup. The beam was operated with a mean beam current of about  $0.5 \mu\text{A}$  and divergence of about  $0.1 \text{ mrad}$ . The target consisting of a  $50 \mu\text{m}$  thick (100) cut silicon crystal was mounted onto a motorised stage which allowed a precise alignment of the crystallographic planes with respect to the beam axis. In the experiment, the crystal was aligned in Laue geometry in two orientations for the observation of the (220) and the (400) reflex family. A detector was placed under the observation angle of  $\Theta_D = 22.5^\circ$ , which corresponds to the first-order PXR photon energies of  $\omega_{220} = 16.55 \text{ keV}$  and  $\omega_{400} = 23.40 \text{ keV}$ , respectively.

The distance between the target and the detector is about 350 mm. A compact high-resolution X-ray camera was used as the detector (ProxiVision HR25 X-ray). It is based on a conventional

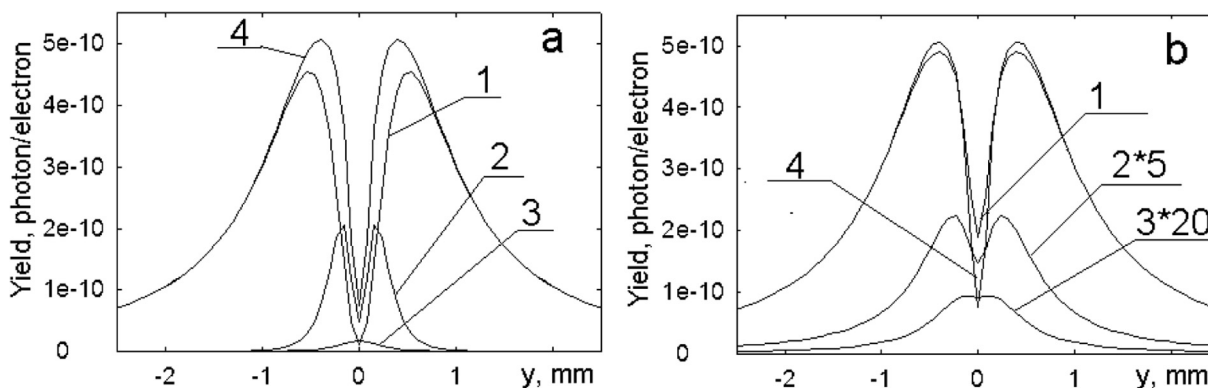


Fig. 1. Spatial distribution of X-ray intensity for (100) reflection plane and the first reflection order in vertical direction (Fig. 1a) and total radiation for three reflection order (Fig. 1b) for the experimental condition of [8].

Download English Version:

<https://daneshyari.com/en/article/5467763>

Download Persian Version:

<https://daneshyari.com/article/5467763>

[Daneshyari.com](https://daneshyari.com)